Mode-locking behavior of Izhikevich neurons under periodic external forcing

AmirAli Farokhniaee[*] and Edward W. Large

Department of Physics and Music Dynamics Laboratory, Department of Psychology,
University of Connecticut, Storrs, Connecticut 06268, USA

Many neurons in the auditory system of the brain must encode periodic signals. These neurons under periodic stimulation display rich dynamical states including mode locking and chaotic responses. Periodic stimuli such as sinusoidal waves and amplitude modulated sounds can lead to various forms of $n : m$ mode-locked states, in which a neuron fires n action potentials per m cycles of the stimulus. Here, we study mode-locking in the Izhikevich neurons, a reduced model of the Hodgkin–Huxley neurons. The Izhikevich model is much simpler in terms of the dimension of the coupled nonlinear differential equations compared with other existing models, but excellent for generating the complex spiking patterns observed in real neurons. We obtained the regions of existence of the various mode-locked states on the frequency-amplitude plane, called Arnold tongues, for the Izhikevich neurons. Arnold tongue analysis provides useful insight into the organization of mode-locking behavior of neurons under periodic forcing. We find these tongues for both class-1 and class-2 excitable neurons in both deterministic and noisy regimes.

I. INTRODUCTION

Mode locking is a ubiquitous phenomenon in the auditory system. Recent research has uncovered evidence of mode locking in single-unit extracellular chopper and onset cells of guinea pigs [1,2], in the auditory midbrain of the fish Pollimyrus in response to acoustic signals [3,4] and in saccular hair bundle cells when exposed to periodic mechanical deflections [5]. To study the mode-locking behavior of a single neuron one must focus on the periodic external forcing (input) and the resulting neuronal spike pattern (output). In the aforementioned studies sinusoidal stimuli were used; therefore, in order to address the phase relations seen in these experiments, one can use sinusoidal current injections into the model neuron and then measure mode-locking behavior by utilizing an Arnold tongue analysis [6,7]. The analysis strategy presented here is tested on the data set that contains the responses of an inferior colliculus neuron in the awake rabbit in response to sinusoidally amplitude modulated (SAM) stimuli across a range of amplitudes and frequencies [8]. This data set was recorded as part of a study to determine physiological responses to SAM stimuli, in which the methods are described in detail [9].

A neuron is said to be $n : m$ mode locked to a periodic stimulus if it fires n action potentials in m cycles of the stimulus, where n and m are positive integers. Phase locking is defined as $1 : 1$ mode locking. For two mode-locked oscillators the locking condition is as follows [10,11]:

$$|\phi_{n,m}| < \text{const.}, \tag{1}$$

where $\phi_{n,m}(t) = n\phi_1(t) - m\phi_2(t)$ and $\phi_{n,m}$ is the generalized phase difference also known as the relative phase. It is clear that in the case when $n = m = 1$ Eq. (1) becomes $|\phi_1(t) - \phi_2(t)| < $ const. This behavior is indicative of constant phase shift, or

phase locking, which is generally considered the simplest way to describe synchronization [11].

To analyze the synchronization of such an oscillator undergoing external forcing, it is constructive to obtain a global map of synchronization regions. Synchronization between a neuron's action potentials or spike trains and an external input depends on both amplitude and frequency of the input. Hence, one can obtain regions on the amplitude-frequency plane that are indicative of mode locking and synchronization of the two signals, i.e., synchronization of the injected periodic signal and the neuronal output. Within these regions, which are commonly referred to as Arnold tongues [11], Eq. (1) holds.

Arnold tongue diagrams have been produced for the Hodgkin–Huxley model [12], oscillators in the canonical model [13], and leaky integrate and fire (LIF) neurons [2]. The analysis of mode-locking for nonlinear oscillators (such as Hodgkin–Huxley) with nonlinear stimuli has been a difficult task [14] and investigators provided the Arnold tongues for such models numerically [12]. Nevertheless, analytical calculation of Arnold tongues have already been done for a simple integrate and fire model [14,15] by using the Poincaré map. We compute the Arnold tongues for the Izhikevich model numerically and present the stability analysis by studying the bifurcations.

This paper utilizes and reports Arnold tongue diagrams for single Izhikevich neurons in both deterministic and stochastic situations. In the presence of noise, synchronization still occurs. However, in order to measure the stability of synchronized states one must introduce a measure. This can be done by using vector strength (VS) so that synchronization can be measured both with and without the presence of noise in this model. VS takes a value of unity if all spikes occur at one precise point and zero for a uniform distribution of phases across the stimulus cycle. VS gives a good indication as to whether a phase preference exists in the data both with and without noise [2]. There have been studies to measure the stability of mode-locked patterns by using different neuronal models, such as Morris–Lecar [16] and LIF neurons [17]. Here

───────
[*]Neuromodulation Laboratory, Department of Biomedical Engineering, School of Medicine, Case Western Reserve University, Cleveland, Ohio, USA; aafarokh@gmail.com

we measure the stability of different mode-locked states by using the Izhikevich model.

In this study, we first explain the neuronal model (Izhikevich 2003) that will be utilized. We then present a brief description of class-1 and class-2 excitable neurons with their corresponding bifurcations. Then we compute the Arnold tongues for the deterministic case and show examples of mode locking. The formation of harmonics and subharmonics in the frequency response of the neuron are then analyzed for some example points in the mode-locking regions. Next, we consider mode-locking in the presence of noise, which more accurately simulates biological conditions. This is done by computing the vector strength to measure the stability of mode-locked regions. The computational tools and analytical methods developed here can also be applied to physiological spike trains for any type or class of neuron.

II. MODEL AND METHODOLOGY

A. Izhikevich model

One of the most significant and influential models in computational neuroscience is the Hodgkin–Huxley model of the squid giant axon [18]. This model captures the generation of action potentials by modeling the inward and outward currents into a neuron through voltage-gated ion channels. In general it consists of four coupled nonlinear differential equations and many parameters that depend on the electrophysiology of the neuron under study. These parameters are usually obtained by experiment.

The spiking model of Izhikevich is a canonical model based on the Hodgkin–Huxley model, with reduced dimensionality. This simple model consists of two coupled nonlinear differential equations that give the time evolution of the components of the system in phase space [18,19]:

$$C\dot{v} = k(v - v_r)(v - v_t) - u + I(t),$$
$$\dot{u} = a[b(v - v_r) - u],$$
$$\text{if } v \geqslant v_{\text{peak}} \text{ then } v \longleftarrow c, \quad u \longleftarrow u + d, \qquad (2)$$

where v is the membrane potential, u is the membrane recovery variable which accounts for the activation of K^+ ionic currents and inactivation of Na^+. u provides negative feedback to v. In this model, C presents the membrane capacitance (in nF), v_r is the resting membrane potential, v_t is the instantaneous threshold potential, and v_{peak} is the spike cutoff value. a is the recovery constant, c is the voltage reset value, and d is the parameter that describes the total flow of ionic current during the spike and affects the after-spike behavior [18]. $I(t)$ is the time-dependent injected current to the neuron that includes a constant part I_{DC}, and an alternating one, $I_{\text{AC}} = A \sin(\omega t)$:

$$I(t) = I_{\text{DC}} + I_{\text{AC}} = I_{\text{DC}} + A \sin(\omega t), \qquad (3)$$

where A is the periodic stimulus amplitude and $\omega = 2\pi f$ with f as the periodic forcing frequency in Hz.

The coefficients are chosen such that both membrane potential v and t are represented in millivolts and milliseconds, respectively. Different values of the parameters a, b, c, d in the model correspond to known types of neurons. This reduced model is derived based on an approximation of Hodgkin–Huxley model nullclines. The Izhikevich model is simple yet
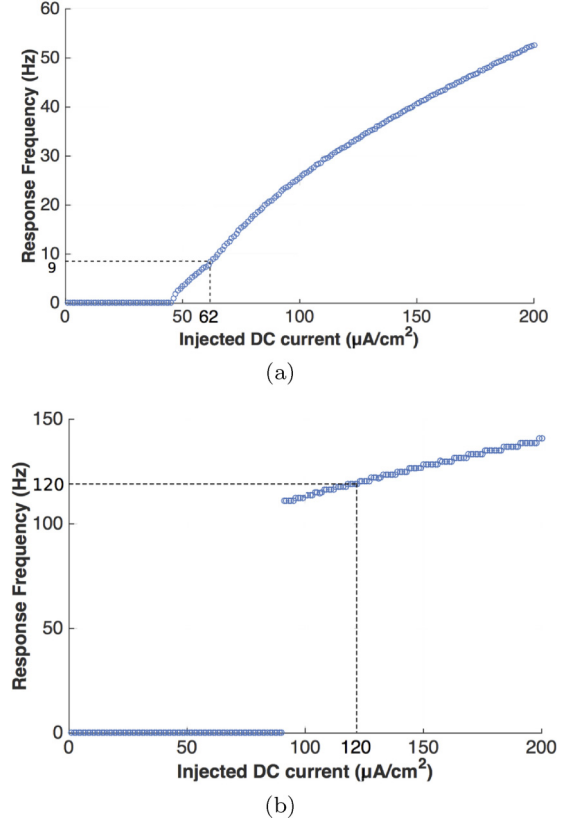

FIG. 1. F-I curves for (a) class-1 and (b) class-2 neurons with parameters given in the text.

incredibly precise and has broad applications to almost all types of neurons. It exhibits firing patterns of *all* known types and is efficient in large-scale simulation of cortical networks [19].

As introduced by Izhikevich [18], the sum of all slow currents that modulate the spike generation mechanism is represented by the phenomenological variable u. Depending on the sign of b, u is either an amplifying (for $b \leqslant 0$) or resonating (for $b \geqslant 0$) variable that defines the class of excitability.

B. Different classes of neurons

A simple but useful criterion for classifying neuronal excitability was suggested by Hodgkin [20]. He discovered by stimulating a cell by applying currents of various strength that when the current was weak the cell was quiet, conversely when the current became strong the cell began to fire repeatedly. Thus, he divided neurons into two classes according to the frequency of emerging firing: class-1 neural excitability, in which action potentials can be generated with arbitrarily low frequency that increases in accordance with the applied current, and class-2 neural excitability, where action potentials are generated in a certain frequency band that is relatively insensitive to changes in the strength of the applied current. These two classes are reproduced by changing the parameters of Izhikevich model, Eqs. (2), in Fig. 1. For both classes of neurons in Fig. 1, $C = 100$ nF, $v_{\text{peak}} = 35$ mV, and $k = 0.7$. For the class-1 neuron with the F-I curve illustrated in Fig. 1(a),

$a = 0.03$, $b = -2$, $c = -50$, $d = 80$, $v_t = -45$ mV, and $v_r = -64$ mV. For the class-2 neuron with the F-I curve shown in Fig. 1(b), $a = 0.1$, $b = 2$, $c = -30$, $d = 100$, $v_t = -40$ mV, and $v_r = -60$ mV.

As described earlier, the sign of b determines the neuron's excitability class, i.e., one can convert from a class-1 model neuron to a class 2 by changing the sign of b. For class-1 neurons, such as the regular spiking cortical pyramidal cells, the resting state disappears through a saddle node on an invariant circle (SNIC) bifurcation. Conversely, for class-2 neurons, such as the fast spiking cortical interneurons, the resting state loses stability via either a saddle node or a subcritical or supercritical Andronov–Hopf bifurcation. One of the reasons for using this classification is its importance and usefulness to understanding the emergence of frequency components of neuronal output (harmonics and subharmonics) which are computed in Sec. III.

III. RESULTS AND ANALYSIS

To study mode-locking we inject the neuron with an external stimulus $I(t) = I_{DC} + A \sin(\omega t)$, as described in Sec. II A. I_{DC} is present to ensure that the neuron spikes. Thus, the value of I_{DC} should be determined by referring to Fig. 1; i.e., it should be selected such that the neuron is in the firing state.

A. Arnold tongue diagram for class-1 neuron

Figure 2 shows the regions of amplitude-frequency plane where different mode-locking ratios can be observed for the class-1 neuron. We computed $n : m$ mode-locked regions for $n,m \in \{1,2,3,4,5\}$. This plot represents the mode-locked regions as a function of the amplitude and frequency of the sinusoidal forcing, with the direct current of $I_{DC} = 62\ \mu A/cm^2$. Note that the $1 : 1$ tongue starts off the x axis at $f = 9$ Hz, the inherent frequency of the class-1 neuron, shown in Fig. 1(a).

As mentioned previously, the $n : m$ ratio is indicative of a mode-locked state. For example, for stimulus amplitudes and frequencies corresponding to the orange region, the neuron exhibits $3 : 1$ mode locking.
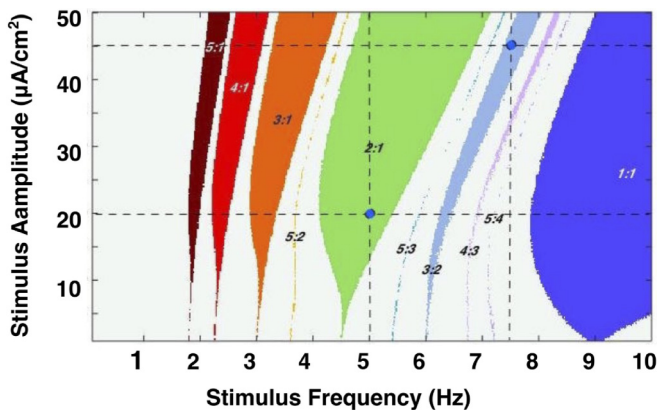

FIG. 2. Arnold tongue diagram for a class-1 Izhikevich neuron with the F-I curve shown in Fig. 1(a), driven by an external sinusoidal forcing. The DC current is $62\ \mu A/cm^2$.
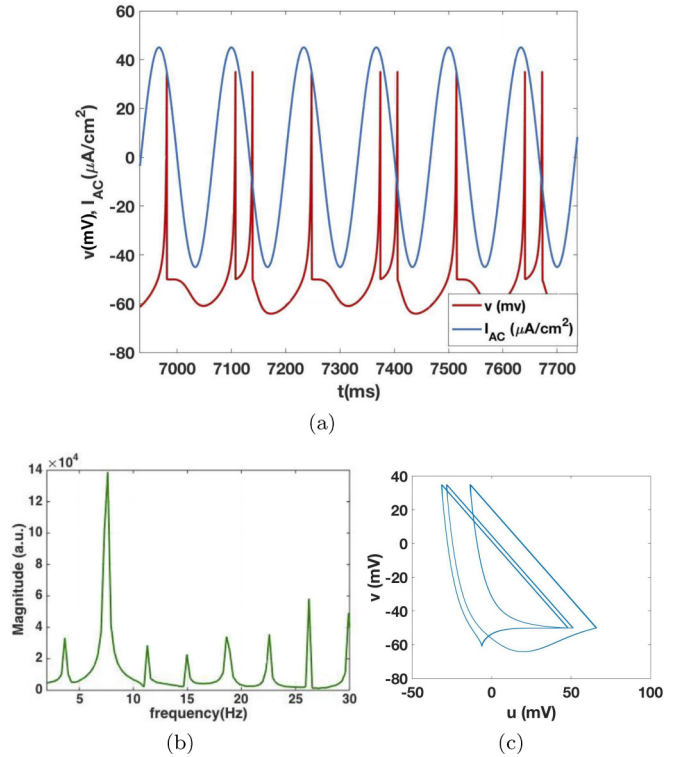

(a)

(b)   (c)

FIG. 3. First example: $3 : 2$ mode-locked pattern.(a) Time series diagram of a sinusoidal stimulus with amplitude of $A = 45\ \mu A/cm^2$ and frequency of $f = 7.5$ Hz (blue) and the corresponding spike pattern (red). (b) Frequency spectrum of the spike pattern. (c) Phase-space diagram.

For each element of the amplitude-frequency matrix that forms the plane, we simulated the model for 10 s. Then in order to have a stable firing pattern of the neuron, the last 5 s of the spiking pattern and corresponding stimulus were considered. If Eq. (1) is satisfied, this particular element takes the value of $n : m$, otherwise it takes zero. The same procedure is done to find the other elements of the matrix and form the whole plane in Figs. 2 and 5. Note that using Eq. (1) in a computer code requires defining a tolerance zone, i.e., the constant value defined on the right-hand side (RHS) can be any number less than a tolerance zone defined by the user.

We demonstrated the time series of the spiking pattern plus the frequency spectrum of the spike trains for the two different points of this diagram which, as previously mentioned, correspond to two different amplitudes and frequencies of the stimulus. For $A = 45\ \mu A/cm^2$ and $f = 7.5$ Hz, we have $3 : 2$ mode locking that is presented in Fig. 3(a). For the corresponding values of A and f, the frequency spectrum of the output has been computed by a Fourier transform and presented in Fig. 3(b) as well. The sharp peak observable in Fig. 3(b) corresponds to the driving frequency of the neuron, i.e., 7.5 Hz. There are peaks as multiples of this driving frequency, which present the input harmonics. Also, there is a smaller ratio of the driving frequency that corresponds to a subharmonic of the input. This example of a $3 : 2$ mode-locking state has a subharmonic frequency of 3.75 Hz which was calculated by dividing the deriving frequency by two (the denominator of the mode-locked state). Figure 3(c)
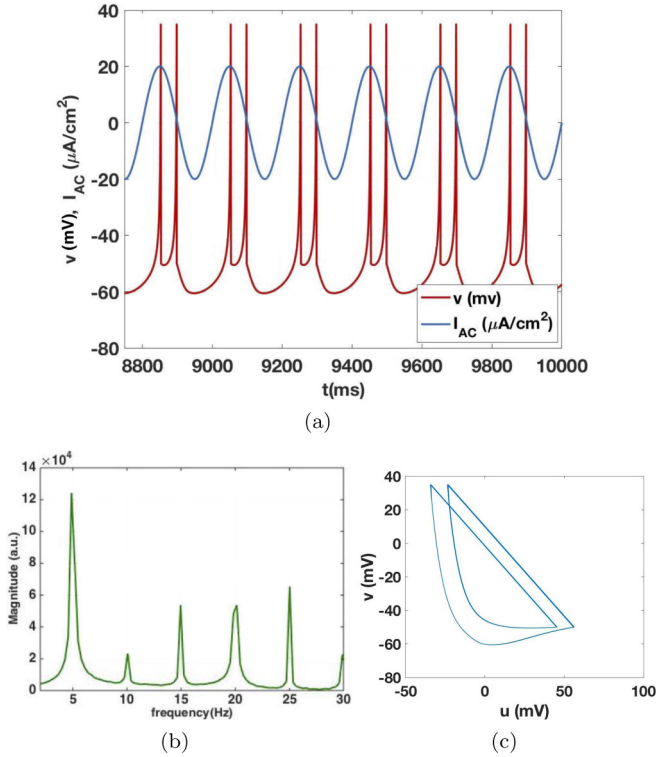
(a)

(b)

(c)

FIG. 4. Second example: 2 : 1 mode-locked pattern. (a) Time series diagram of a sinusoidal stimulus with amplitude of $A = 20 \ \mu\mathrm{A/cm}^2$ and frequency of $f = 5$ Hz (blue) and the corresponding spike pattern (red). (b) Frequency spectrum of the spike pattern. (c) Phase-space diagram.

shows phase-space trajectories of the system for the above selection of A and f.

Another example is $A = 20 \ \mu\mathrm{A/cm}^2$ and $f = 5$ Hz. The corresponding input-output time series and frequency spectrum of the output can be seen in Fig. 4. The formation of harmonics can be observed in Fig. 4(b). However, there are no subharmonics observed here since the denominator of the mode-locked state is unity. Figure 4(c) shows phase-space trajectories of the system for this particular example.

B. Arnold tongue diagram for class-2 neuron

Next, we compute Arnold tongues for the class-2 neuron; Fig. 5. Note that the 1 : 1 tongue initiates at $f = 120$ Hz from the x axis, the inherent frequency of the class-2 neuron [refer to Fig. 1(b)]. In class-2 neurons, action potentials are generated in a certain frequency band, which are not highly dependent on the applied current [Fig. 1(b)]. Hence, the tongues in Fig. 5 are not tilted as much as those in Fig. 2. Furthermore, the tongues occur at relatively higher frequencies (refer to x axis) than the for the class-1 neuron. This is consistent with the fast spiking behavior of class-2 neurons; Fig. 1(b).

Again we consider two example points of this diagram in order to visualize the mode-locked behavior. The corresponding time series and frequency spectra along with phase-space diagrams are given in Figs. 6 and 7.

Note the formation of harmonics and subharmonics again. The amplitude of subharmonics are much greater and more
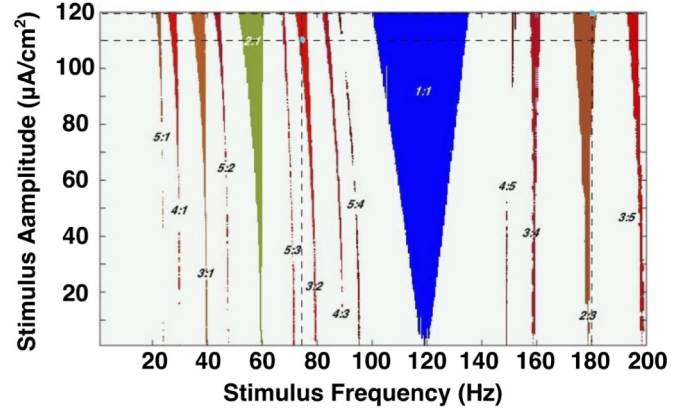

FIG. 5. Arnold tongues diagram for a class-2 Izhikevich neuron driven by an external sinusoidal forcing that corresponds to the neuron with the F-I curve and parameters shown in Fig. 1(b). The DC current is 120 $\mu\mathrm{A/cm}^2$.

dominant than those seen in class-1 neurons. In Fig. 6(b) we have a subharmonic of the driving frequency 37.5 Hz, which corresponds to 75/2 (driving frequency divided by the denominator of the mode-locked state). In the case of Fig. 7(b), which depicts the mode-locked region of 2 : 3 (smaller than 1), subharmonic construction is even more dominant than in the case of Fig. 6(b); additionally it is also greater in amplitude
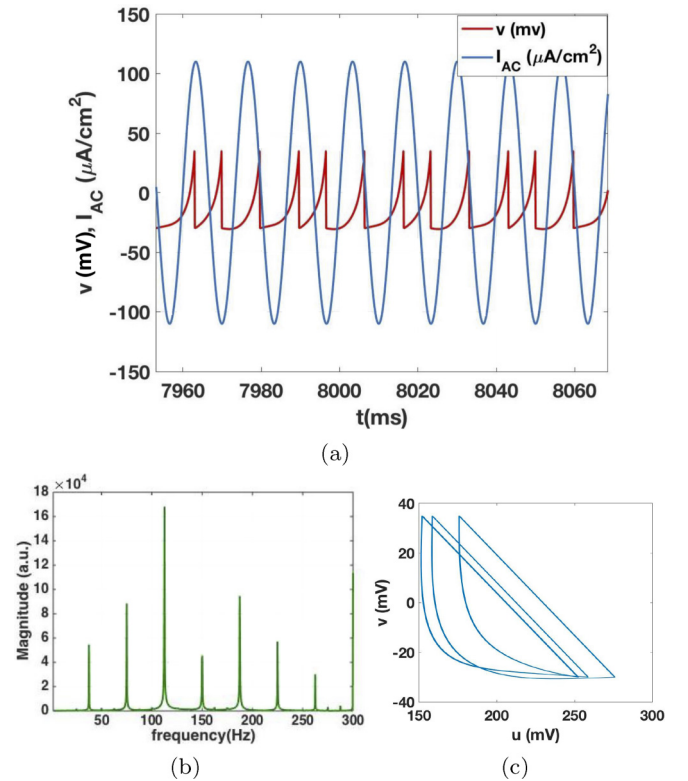

(a)

(b)

(c)

FIG. 6. First example: 3 : 2 mode-locked pattern.(a) Time series diagram of a sinusoidal stimulus with amplitude of $A = 110 \ \mu\mathrm{A/cm}^2$ and frequency of $f = 75$ Hz (blue) and the corresponding spike pattern (red). (b) Frequency spectrum of the spike pattern. (c) Phase-space diagram.
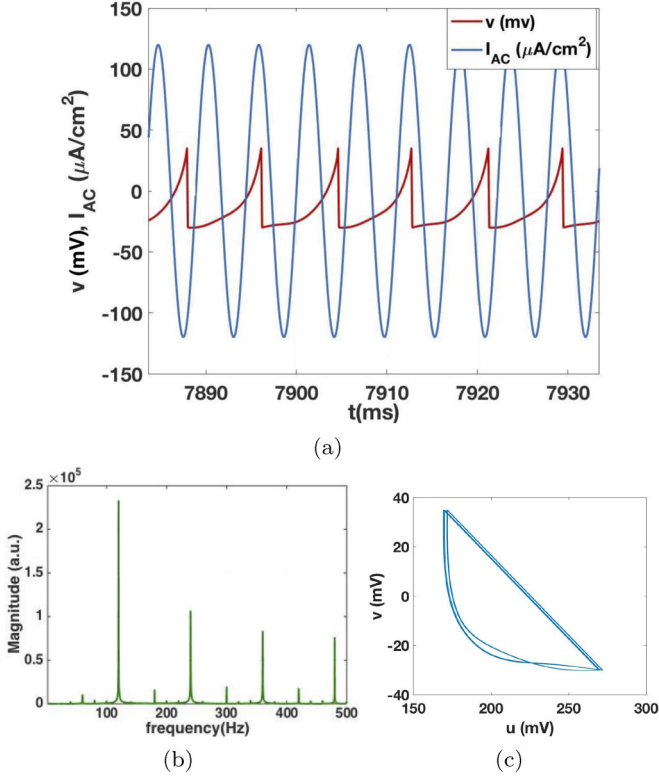
(a)

(b)

(c)

FIG. 7. Second example: 2 : 3 mode-locked pattern. (a) Time series diagram of a sinusoidal stimulus with amplitude of $A = 120$ μA/cm^2 and frequency of $f = 180$ Hz (blue) and the corresponding spike pattern (red). (b) Frequency spectrum of the spike pattern. (c) Phase-space diagram.

(a)

(b)

FIG. 8. (a) Time series and (b) phase-space diagram of the system corresponding to $A = 110$ μA/cm^2 and $f = 36$ Hz in the class-2 neuron. Referring to Fig. 5 shows this selection of stimulus parameters leads to 3 : 1 mode locking. This can be seen also in the solution and formation of limit cycle here.

than the subsequent harmonics. In Fig. 7(b) we have two observed subharmonics at 60 and 120 Hz. The first one is the driving frequency divided by 3 ($180/3 = 60$ Hz) and the second one is $2 \times 60 = 120$ Hz, since the numerator of the mode-locked state is two.

As has been previously studied [18,21,22], class-1 and class-2 neurons differ in the way they respond to input. In class-1 neurons, whose quiescent state disappears through a SNIC bifurcation, the neuron can fire with an arbitrarily low frequency. Conversely, in class-2 neurons the resting potential loses stability via either a saddle node or a subcritical or supercritical Andronov–Hopf bifurcation; i.e., the neuron acts similarly to a bandpass filter in that it extracts the frequencies which correspond to resonant frequencies. This information can be related to our observations and help explain why subharmonics formation in class-2 neurons can be more dominant than in class-1 neurons. The small amplitude oscillations make the neurons to resonate to the driving frequency. The firing frequencies given in F-I curves (Fig. 1) depend on factors beside the type of bifurcation of the resting state [18].

At Arnold tongues boundaries, our system undergoes a state transition at a slight change of amplitude or frequency of the periodic stimulus. Plotting phase-space trajectories helps us understand the transient oscillations of the system between these regions.
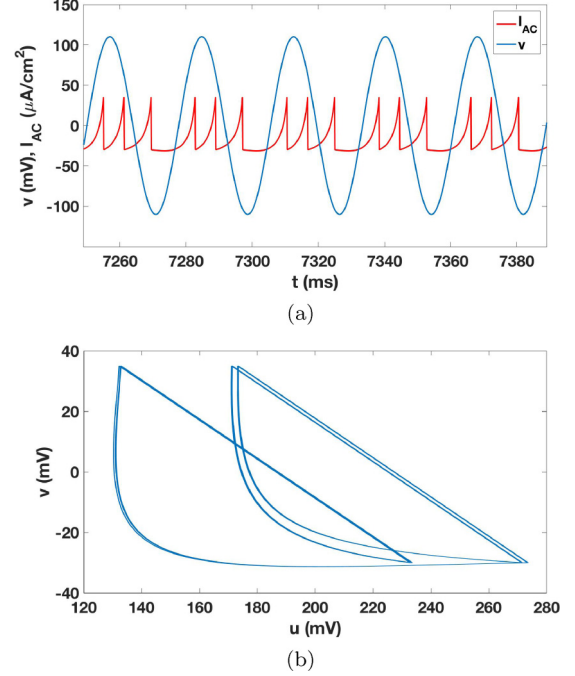
As an example, we select $A = 110$ μA/cm^2 and $f = 36$ Hz in Fig. 5 that corresponds to 3 : 1 mode locking. Figure 8 shows solutions of the system in time domain and phase space at this particular state. Mode-locking corresponds to stable solutions that are also true for the next successive periods. Now we slightly displace the system from this stable solution by changing the stimulus frequency to 35 Hz. The solutions in time domain and phase space are shown in Fig. 9. This solution is not stable anymore, which leads to disappearance of mode locking. The phase-space diagrams suggest an unstable limit cycle with spiral focus that leads to transient oscillations in class-2 neuron and explains the formation of strong subharmonics.

C. Computing Arnold tongues based on vector strength

The methods used to compute Arnold tongues in Figs. 2 and 5 work well for the deterministic model [system of Eqs. (2)]. However, they begin to break down when noise is applied to the model. We use the spiking model of Izhikevich with the additive white Gaussian noise $\eta(t)$, which has a normal distribution with zero mean $\mu = 0$, and the variance σ^2:

$$C\dot{v} = k(v - v_r)(v - v_t) - u + I(t) + \eta(t),$$

$$\dot{u} = a[b(v - v_r) - u],$$

$$\text{if } v \geqslant v_{\text{peak}} \text{ then } v \longleftarrow c, \quad u \longleftarrow u + d.$$

The level of noise in our following simulations is varied by changing the value of σ^2, which consequently creates different noisy regimes of the system under study.
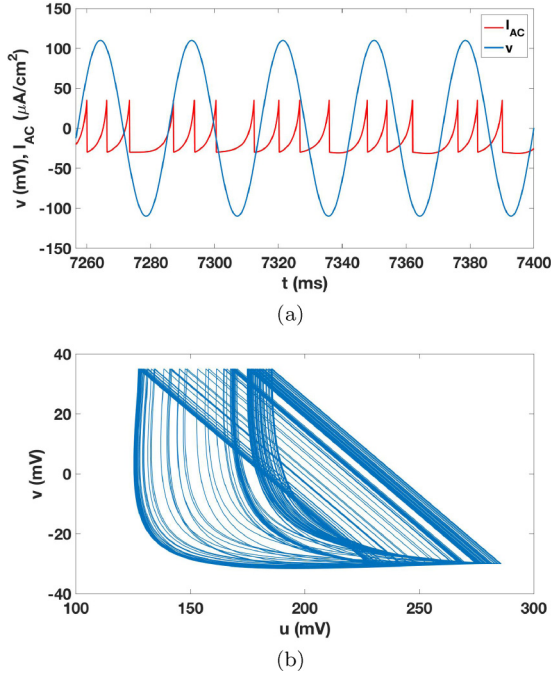
(a)

(b)

FIG. 9. (a) Time series and (b) phase-space diagram of the system corresponding to $A = 110$ μA/cm^2 and $f = 35$ Hz in the class-2 neuron. The solution is not stable any more, which leads to disappearance of mode-locking and periodic decay in phase space.

In addressing this more realistic situation we consider vector strength (VS). As mentioned previously, VS takes on a value near unity when the neuronal spike events always occur at the same phase of the stimulus and vanishes for equally distributed spike times.
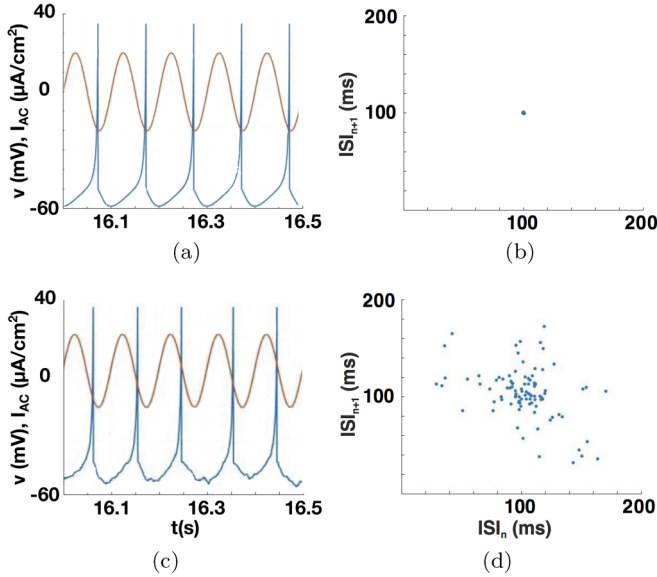

(a)

(b)

(c)

(d)

FIG. 10. (a) Spike trains of a $1:1$ mode-locked state without noise and (b) the corresponding ISIs. (c) After adding the white Gaussian noise with $\mu = 0$ and $\sigma^2 = 5$, the mode-locking pattern becomes less stable and (d) the corresponding ISIs no longer overlap on a well-defined point.
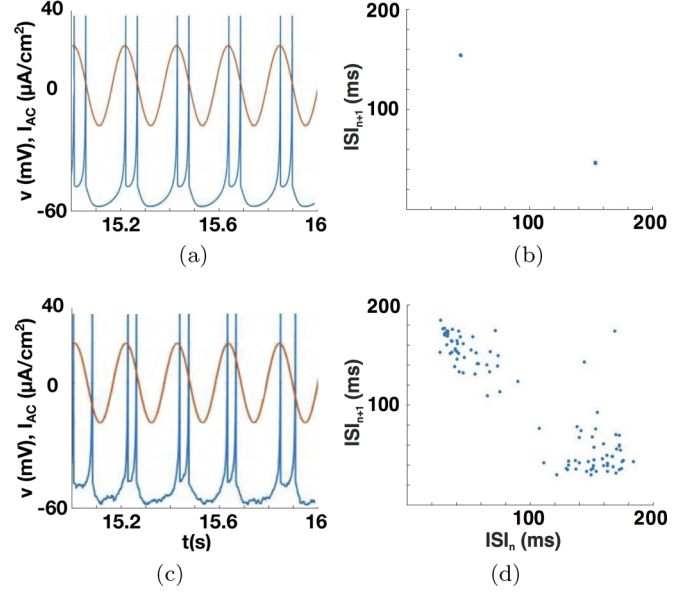

(a)

(b)

(c)

(d)

FIG. 11. (a) Spike trains of a $2:1$ mode-locked state without noise and (b) the corresponding ISIs. (c) After adding the white Gaussian noise with $\mu = 0$ and $\sigma^2 = 5$, the mode-locking pattern becomes less stable and (d) the corresponding ISIs no longer overlap on two well-defined points.

Vector strength quantifies the amount of periodicity in the neuronal response to a given periodic signal. The neural response is denoted by a sequence of spike times $\{t1, t2, \dots, tn\}$ where in general $n \gg 1$. t_j is defined for $1 \leqslant j \leqslant n$. VS is the length of the synchrony vector [23]:

$$\text{VS} = \frac{1}{n} \left| \sum_{j=1}^{n} e^{-i\omega t_j} \right|. \qquad (4)$$

Here, $\omega = \frac{2\pi}{T}$ denotes an angular frequency for some period T. Equation (4) transforms the spike times t_j or, more precisely, the dimensionless times t_j/T, onto a circle with radius 1.

The advantage of using VS-based Arnold tongues is that it can be used for the noisy model. However, there exists the fundamental problem that VS can only be used to analyze $1:1$ mode locking [10]. Nevertheless, we suggest an idea that lets us extend this method to all mode-locked states
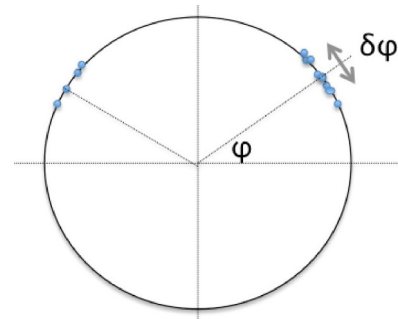

FIG. 12. The unit circle that is used to find the smallest phase ϕ. The window $\delta\phi$ is defined by the user and indicates the radius of the cluster under study in the ISIs; Fig. 11(d).
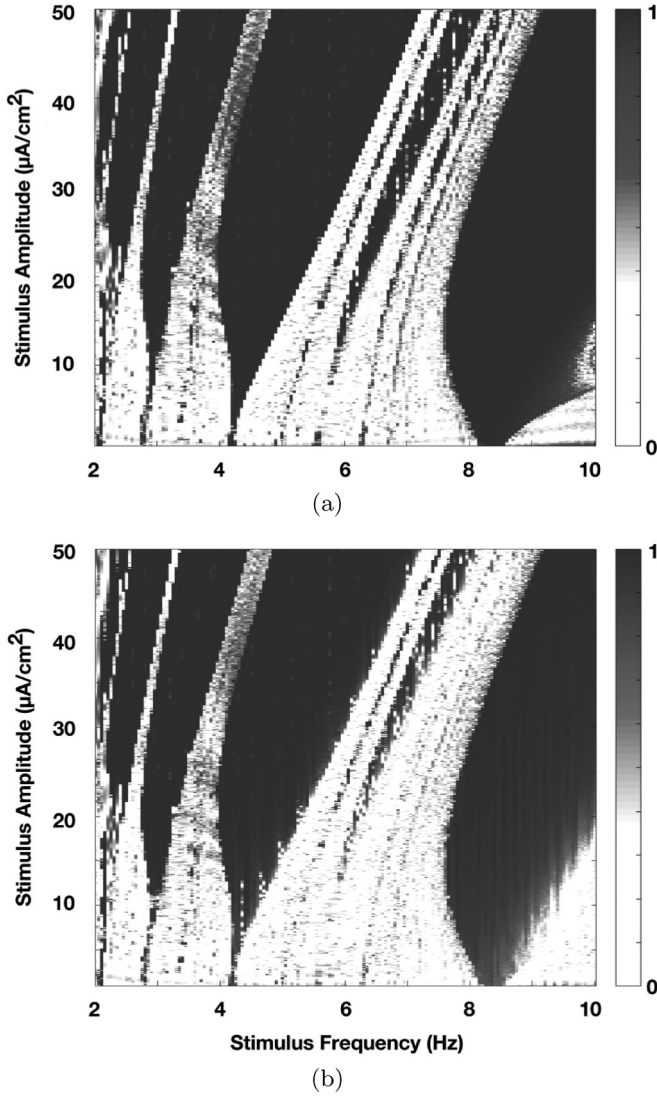
FIG. 13. VS-based Arnold tongue diagram of the class-1 neuron in the presence of noise with different strengths (a) $\mu = 0$, $\sigma^2 = 2$ and (b) $\mu = 0$, $\sigma^2 = 5$. Time step for computing the Izhikevich model is 0.05 ms. The color code represents the amount of vector strength. Note how the different mode-locked states lose their stabilities with the addition of noise compared with Fig. 2.
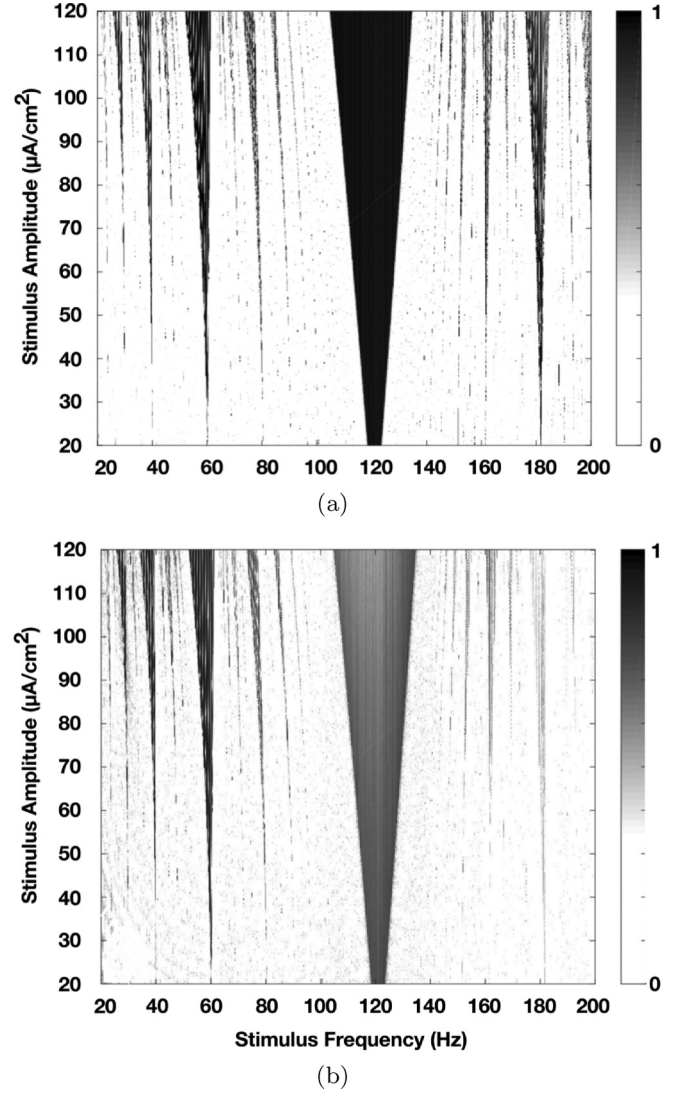
FIG. 14. VS-based Arnold tongue diagram of the class-2 neuron in the presence of noise with different strengths (a) $\mu = 0$, $\sigma^2 = 2$ and (b) $\mu = 0$, $\sigma^2 = 5$. Time step for computing the Izhikevich model is 0.05 ms. The color code represents the amount of vector strength. Note how the different mode-locked states lose their stabilities with the addition of noise compared with Fig. 5.

by considering the pattern existence, i.e., to use Eq. (4) by substituting the time of the first spike per period. Using VS in this way is akin to 1 : 1 mode-locking analysis and can be done by looking at the interspike intervals.

Interspike intervals (ISI $= t_{j+1} - tj$) can be plotted successively so that they form ISI return maps. Figures 10 and 11 show some examples of these maps for different mode-locked states and their corresponding spike trains. If the model is deterministic (no noise), the clusters shrink to the number of points corresponding to the denominator of the mode-locking ratio, m periods of stimulus. In the presence of noise, however, there tends to be clusters of points bound in regions around the deterministic points. The boundaries around these points can be defined in a way that yields the area of clusters depending on the level of noise. This allows us to compute the mode-locked regions in the presence of

noise. Smaller clusters result in bigger VS and consequently, the stability of the mode-locked state is higher.

The number of clusters tells us the denominator of the mode-locking ratio. We chose only one of the clusters, and then measured VS over the whole time of recording only for that cluster. The method to choose the preferred cluster in ISI return maps is analogous to selecting the preferred phase around a mean value on a circle defined by a radius that has a magnitude equal to VS. Figure 12 shows the phase analog of the ISIs in Fig. 11(d). We find the mean value of the smaller angle ϕ, which corresponds to the center of one of the clusters by $\phi = \omega t$ and choose a window $\delta\phi$ that is defined by the user. This $\delta\phi$ is related to the radius of the already-chosen cluster by $\delta\phi = \omega \delta t$. Note that we are allowed to do this since the relationship between the angle ϕ and time t is linear. In this case, even under noisy conditions there will still be
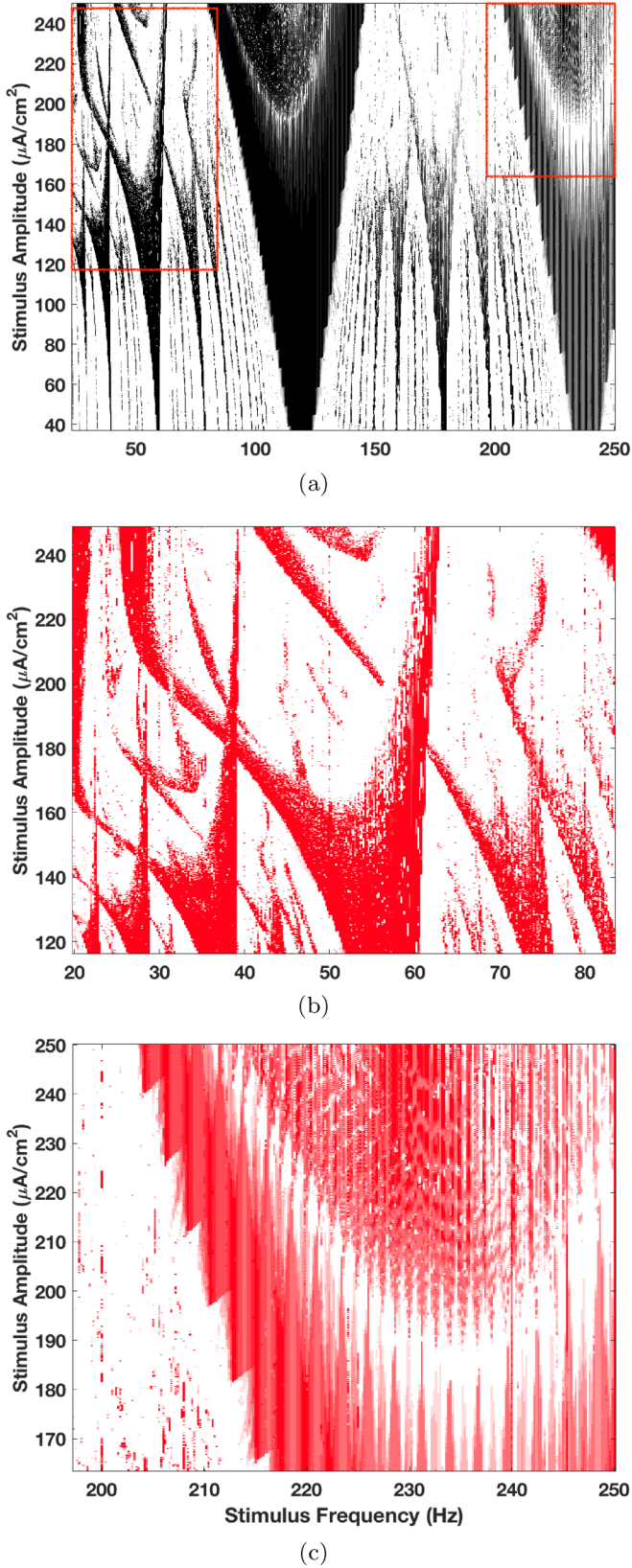
(a)

(b)

(c)

FIG. 15. (a) Arnold tongues for the noisy class-2 neuron in a broader range of amplitude and frequency of periodic stimulus. (b) Zoomed-in region on the left side of panel (a) shown with a red rectangle. The tongues are entangled at high amplitudes. (c) Zoomed-in part of 1 : 2 tongue shown with a red rectangle in panel (a).

synchronization, albeit with less stability than the deterministic model.

Figure 13 illustrates the evaluated Arnold tongues based on the VS concept for the noisy class-1 neuron in two different noise regimes. In the same fashion we obtained VS-based Arnold tongues for the noisy class-2 neuron in Fig. 14. In the presence of noise (Figs. 13 and 14), it is observed that the tongue edges (boundaries) become less distinct and some of the tongues (e.g., 5 : 4) completely disappear. In this process it appears that the tongues corresponding to $n : m$ mode-locked states with $n > m$ are more stable than those with $n < m$.

Figure 15(a) represents Arnold tongues for the noisy class-2 neuron as in Fig. 14(a) but with the broader range of amplitude and frequency of the periodic external forcing.

Arnold tongues on the left-hand side of the diagram that are shown with the red rectangle, entangle for higher amplitudes. A zoomed-in map is presented in Fig. 15(b). The entanglement of these tongues leads to chaotic behavior of the neuron.

It appears that the mode-locked region boundaries harbor a fine structure. A more detailed structure of the 1 : 2 tongue is shown in Fig. 15(c). Also, there are substructures within the 2 : 1 tongue and similarly for other tongues. The stability and creation of substructures within the boundary depends on the amount of noise.

IV. CONCLUSION

Computational techniques used to investigate mode locking have become an important tool in the analysis of synchronization. Recent investigations into periodic forcing have provided a wealth of information regarding the processing of temporal information and the characteristics of synchronization [12,24]. Arnold tongues and other bifurcation structures in phase space can help us explain the neuronal behavior seen in auditory signal processing neurons such as those in the cochlear nucleus (CN) [2] and inferior colliculus (IC) [8].

By using Izhikevich neurons, we constructed a deterministic model which simulates the mode locking of a single neuron to external sinusoidal forcing. However, real neurons have noisy responses. Traditional approaches cannot be directly applied here, so we slightly adjusted the vector strength method in order to account for the stochastic nature of the system. By employing this method, we constructed Arnold tongue diagrams for a stochastic system in which we examined how the presence of noise influenced the degree to which mode-locking was observed. This is of importance because neural encoding in the auditory system is inherently noisy [3,7,25]. Inner hair cell (IHC) receptor potentials follow oscillatory motion but are low-pass filtered [5,25]. There is stochastic neurotransmitter release between IHC and auditory nerve (AN) fibers and the resulting action potentials reflect the time-varying nature of IHC membrane oscillations. AN fibers project to CN of the brainstem. The stellate cells in CN include choppers and onsets which differ in timing of the firing in response to periodic stimuli. This sensory coding includes the mode-locking phenomenon and is also observable in higher levels of the auditory system such as the IC [8,9].

To understand and address these complex interactions, Arnold tongue diagrams of the aforementioned cells give us a global map in parameter space that could be used to justify

the observations. We have specifically utilized Arnold tongue diagrams for the Izhikevich model presented in this study to help in the understanding of the organization of the responses to SAM tones across a range of amplitudes and frequencies [8], for a given set of data that is recorded from the IC cells of an awake rabbit [9].

[1] D. C. Bullock, A. R. Palmer, and A. Rees, Compact and easy-to-use tungsten-in-glass microelectrode manufacturing workstation, Med. Biol. Eng. Comput. **26**, 669 (1988).

[2] J. Laudanski, S. Coombes, A. R. Palmer, and C. J. Sumner, Mode-locked spike trains in responses of ventral cochlear nucleus chopper and onset neurons to periodic stimuli, J. Neurophysiol. **103**, 1226 (2010).

[3] E. W. Large and J. D. Crawford, Auditory temporal computation: Interval selectivity based on post-inhibitory rebound, J. Comput. Neurosci. **13**, 125 (2002).

[4] E. W. Large and F. V. Almonte, Neurodynamics, tonality, and the auditory brainstem response, Ann. N. Y. Acad. Sci. **1252**, E1 (2012).

[5] L. Fredrickson-Hemsing, S. Ji, R. Bruinsma, and D. Bozovic, Mode-locking dynamics of hair cells of the inner ear, Phys. Rev. E **86**, 021915 (2012).

[6] P. X. Joris, C. E. Schreiner, and A. Rees, Neural processing of amplitude-modulated sounds, Physiol Rev. **84**, 541 (2004).

[7] K. D. Lerud, F. V. Almonte, J. C. Kim, and E. W. Large, Mode-locking neurodynamics predict human auditory brainstem responses to musical intervals, Hear. Res. **308**, 41 (2014).

[8] AmirAli Farokhniaee, Ph.D. thesis, University of Connecticut, 2016 (unpublished).

[9] L. H. Carney, M. S. A. Zilany, N. J. Huang, K. S. Abrams, and F. Idrobo, Suboptimal use of neural information in a mammalian auditory system, J. Neurosci. **34**, 1306 (2014).

[10] P. Tass, M. G. Rosenblum, J. Weule, J. Kurths, A. Pikovsky, J. Volkmann, A. Schnitzler, and H. J. Freund, Detection of *n*:*m* Phase Locking from Noisy Data: Application to Magnetoencephalography, Phys. Rev. Lett. **81**, 3291 (1998).

[11] A. Pikovsky, M. Rosenblum, and J. Kurts, *Synchronization: A Universal Concept in Nonlinear Sciences*, Cambridge Nonlinear Science Series 12 (Cambridge University Press, New York, 2001).

[12] S. G. Lee and S. Kim, Bifurcation analysis of mode-locking structure in a Hodgkin–Huxley neuron under sinusoidal current, Phys. Rev. E **73**, 041924 (2006).

[13] J. C. Kim and E. W. Large, Signal processing in periodically forced gradient frequency neural networks, Front. Comput. Neurosci. **9**, 152 (2015).

[14] L. Glass and M. C. Mackey, A simple model for phase locking of biological oscillators, J. Math. Biol. **7**, 339 (1979).

[15] L. Glass, Synchronization and rhythmic process in physiology, Nature (London) **410**, 277 (2001).

[16] M. Oh and V. Matveev, Loss of phase-locking in non-weakly coupled inhibitory networks of type-*i* model neurons, J. Comput. Neurosci. **26**, 303 (2009).

[17] T. J. Lewis and J. Rinzel, Dynamics of spiking neurons connected by both inhibitory and electrical coupling, J. Comput. Neurosci. **14**, 283 (2003).

[18] E. M. Izhikevich, *Dynamical Systems in Neuroscience* (The MIT Press, Cambridge, MA, 2007).

[19] E. M. Izhikevich, Simple model of spiking neurons, IEEE Trans. Neural Networks **14**, 1569 (2003).

[20] A. L. Hodgkin, The local electric changes associated with repetitive action in a non-medullated axon, J. Physiol. **107**, 165 (1948).

[21] F. C. Hoppensteadt and E. M. Izhikevich, *Weakly Connected Neural Networks*, Applied Mathematical Sciences (Springer, New York, 1997), Vol. 126.

[22] E. M. Izhikevich, Neural excitability, spiking and bursting, Int. J. Bifurcation Chaos Appl. Sci. Eng. **10**, 1171 (2000).

[23] J. L. van Hemmen, A. Logtin, and A. N. Vollmayr, Testing resonating vector strength: Auditory system, electric fish, and noise, Chaos **21**, 047508 (2011).

[24] Y. Kim, Identification of dynamical states in stimulated Izhikevich neuron models by using a 0-1 test, J. Korean Phys. Soc. **57**, 1363 (2010).

[25] S. Coombes, R. Thul, J. Laudanski, A. R. Palmer, and C. J. Sumner, Neuronal spike-train responses in the presence of threshold noise, Front. Life Sci. **5**, 91 (2011).